

Light Relic Neutralinos*

A. Bottino,^{1,†} N. Fornengo,^{1,‡} and S. Scopel^{1,§}

¹*Dipartimento di Fisica Teorica, Università di Torino
Istituto Nazionale di Fisica Nucleare, Sezione di Torino
via P. Giuria 1, I-10125 Torino, Italy*

(Dated: November 5, 2018)

The relic abundance and the scalar cross-section off nucleon for light neutralinos (of mass below about 45 GeV) are evaluated in an effective MSSM model without GUT-inspired relations among gaugino masses. It is shown that these neutralinos may provide a sizeable contribution to the matter density in the Universe and produce measurable effects in WIMP direct detection experiments. These properties are elucidated in terms of simple analytical arguments.

PACS numbers: 95.35.+d,11.30.Pb,12.60.Jv,95.30.Cq

I. INTRODUCTION

Most works on relic neutralinos consider supersymmetric schemes with a unification assumption for the gaugino masses M_i ($i = 1, 2, 3$) at the GUT scale $M_{GUT} \sim 10^{16}$ GeV. This hypothesis implies that at lower scales the following relations hold:

$$M_1 : M_2 : M_3 = \alpha_1 : \alpha_2 : \alpha_3, \quad (1)$$

where the α_i ($i = 1, 2, 3$) are the coupling constants of the three Standard Model gauge groups. In particular, at the electroweak scale, $M_{EW} \sim 100$ GeV, M_1 and M_2 are related by the expression:

$$M_1 = \frac{5}{3} \tan^2 \theta_W M_2 \simeq 0.5 M_2. \quad (2)$$

However, there are theoretical arguments for considering supersymmetric schemes where the unification assumption on gaugino masses is not satisfied[1].

In the present paper we analyse properties of relic neutralinos in an effective Minimal Supersymmetric extension of the Standard Model (MSSM) where the GUT relation of Eq. (2) is relaxed. Previous papers where supersymmetric schemes without gaugino masses unification have been considered in connection with relic neutralinos include the ones reported in Refs. [2, 3, 4, 5, 6, 7, 8, 9, 10, 11, 12, 13]. Here we evaluate the neutralino relic abundance $\Omega_\chi h^2$ and the neutralino-nucleon scalar cross-section $\sigma_{\text{scalar}}^{(\text{nucleon})}$, which is relevant to dark matter direct detection. In Sect. II we define the supersymmetric scheme adopted in the present paper and in Sect. III we provide analytical considerations and numerical evaluations. Our conclusions are drawn in Sect. IV.

II. EFFECTIVE MSSM WITHOUT GAUGINO UNIFICATION

We employ an effective MSSM scheme (effMSSM) at the electroweak scale, defined in terms of a minimal number of parameters, only those necessary to shape the essentials of the theoretical structure of MSSM and of its particle

*Preprint number: DFTT 42/2002

†Electronic address: bottino@to.infn.it; URL: <http://www.to.infn.it/astropart>

‡Electronic address: fornengo@to.infn.it; URL: <http://www.to.infn.it/astropart>; URL: <http://www.to.infn.it/~fornengo>

§Electronic address: scopel@to.infn.it; URL: <http://www.to.infn.it/astropart>

content. The assumptions that we impose at the electroweak scale are: a) all squark soft-mass parameters are taken degenerate: $m_{\tilde{q}_i} \equiv m_{\tilde{q}}$; b) all slepton soft-mass parameters are taken degenerate: $m_{\tilde{l}_i} \equiv m_{\tilde{l}}$; c) all trilinear parameters are set to zero except those of the third family, which are defined in terms of a common dimensionless parameter A : $A_{\tilde{b}} = A_{\tilde{t}} \equiv Am_{\tilde{q}}$ and $A_{\tilde{\tau}} \equiv Am_{\tilde{l}}$. As a consequence, the supersymmetric parameter space consists of the following independent parameters: $M_2, \mu, \tan\beta, m_A, m_{\tilde{q}}, m_{\tilde{l}}, A$ and $R \equiv M_1/M_2$. In the previous list of parameters we have denoted by μ the Higgs mixing mass parameter, by $\tan\beta$ the ratio of the two Higgs v.e.v.'s and by m_A the mass of the CP-odd neutral Higgs boson.

This scheme differs from the effMSSM which we employed for instance in Ref. [14] in the fact that we are relaxing here the gaugino unification relation, which was instead assumed in our previous works. The presence of the extra R parameter accounts for this fact.

The neutralino is defined as the lowest-mass linear superposition of bino \tilde{B} , wino $\tilde{W}^{(3)}$ and of the two higgsino states $\tilde{H}_1^\circ, \tilde{H}_2^\circ$:

$$\chi \equiv a_1 \tilde{B} + a_2 \tilde{W}^{(3)} + a_3 \tilde{H}_1^\circ + a_4 \tilde{H}_2^\circ. \quad (3)$$

Due to well-known properties of the neutralino and chargino mass matrices, one has that: a) for $\mu \gg M_1, M_2$ the neutralino mass is determined by the lightest gaugino mass parameter: $m_\chi \simeq \min(M_1, M_2)$, while the lightest chargino mass is set by M_2 : $m_{\chi^\pm} \simeq M_2$ (M_1 does not enter the chargino mass matrix at tree-level); b) for $\mu \ll M_1, M_2$ both the neutralino and the chargino masses are primarily set by the Higgs mixing parameter: $m_\chi \simeq \mu \simeq m_{\chi^\pm}$.

LEP data put a stringent lower bound on the chargino mass: $m_{\chi^\pm} \gtrsim 103$ GeV, which converts into lower bounds on M_2 and μ : $M_2, \mu \gtrsim 103$ GeV. This implies a lower bound on the neutralino mass of the order of about 50 GeV in the standard effMSSM, where the GUT relation of Eq.(2) holds. On the contrary, the neutralino mass may be smaller when $M_1 \ll M_2$, thus for small values of the parameter R .

In the present paper we are interested in the phenomenology of light neutralinos, therefore we consider values of R lower than its GUT value: $R_{GUT} \simeq 0.5$. For definiteness we will consider the range: 0.01 - 0.5. The ensuing light neutralinos have a dominant bino component; a deviation from a pure bino composition is mainly due to a mixture of \tilde{B} with \tilde{H}_1° , as will be shown in Sect.III B.

In our numerical analysis we have varied the MSSM parameters within the following ranges: $1 \leq \tan\beta \leq 50$, $100 \text{ GeV} \leq |\mu|, M_2, m_{\tilde{q}}, m_{\tilde{l}} \leq 1000$ GeV, $\text{sign}(\mu) = -1, 1$, $90 \text{ GeV} \leq m_A \leq 1000$ GeV, $-3 \leq A \leq 3$, for a sample of representative values of R in the range $0.01 \leq R \leq 0.5$. This range for R , implemented with the experimental lower limit on M_2 of about 100 GeV, implies that the lower bound on the neutralino mass can be moved down to few GeV's for $R \sim 0.01$.

We then implemented the following experimental constraints: accelerators data on supersymmetric and Higgs boson searches (CERN e^+e^- collider LEP2 [15] and Collider Detector CDF at Fermilab [16]); measurements of the $b \rightarrow s + \gamma$ decay [17]. We wish to comment that the accelerator limits on the Higgs sector are taken into account by implementing the limits on the Higgs production cross-sections: $e^+e^- \rightarrow hZ$ and $e^+e^- \rightarrow hA$ (h and A are the lightest scalar and the pseudoscalar neutral Higgs bosons, respectively), which in turn imply a constraint on the coupling constants $\sin^2(\alpha - \beta)$ and $\cos^2(\alpha - \beta)$. Once these limits are applied, the absolute lower limit on the Higgs masses is $m_A, m_h \sim 90$ GeV. The allowed light-Higgs mass range between 90 and 114 GeV is very often overlooked in studies of neutralino dark matter, where a flat limit of 114 GeV is applied to m_h . The light-Higgs mass range, even though difficult (but not impossible) to be achieved in SUGRA models [18, 19, 20], is nevertheless quite natural in the effMSSM and usually provides large detection rates for neutralino dark matter [19].

As for the constraint due to the muon anomalous magnetic moment $a_\mu \equiv (g_\mu - 2)/2$ we have used the interval $-160 \leq \Delta a_\mu \cdot 10^{11} \leq 680$, where Δa_μ is the deviation of the current world average of the experimental determinations (dominated by the measurements of Ref. [21]) from the theoretical evaluation within the Standard Model: $\Delta a_\mu \equiv a_\mu^{\text{expt}} - a_\mu^{\text{SM}}$. The range we use for Δa_μ is a 2σ interval, obtained by using for the lowest-order hadronic vacuum polarization contribution an average between the results derived from the $e^+ - e^-$ data [22, 23] and from hadronic τ decays [22]. The Δa_μ constraint and the $b \rightarrow s + \gamma$ bound set stringent limits for the light neutralino sector of our models.

Once also the relic abundance bound $\Omega_\chi h^2 \leq 0.3$ is applied (see Sect.III B) in addition to the other experimental constraints discussed above, a lower limit of about 6 GeV is obtained for the neutralino mass in the class of models

with non-universal gaugino masses considered in this paper¹.

III. NEUTRALINO RELIC ABUNDANCE AND NEUTRALINO-NUCLEON CROSS-SECTION

A. Some analytical properties for small m_χ

The neutralino configurations which provide the highest values of direct detection rates are the ones dominated by (h, H) Higgs-exchange processes, which in turn require a gaugino-higgsino mixing. For these configurations, also the relic abundance is regulated by a (A) Higgs-exchange diagram in the $\chi - \chi$ annihilation cross-section.

Thus, to get an insight into the properties to be expected for our light neutralinos we limit ourselves to the following approximate expressions, derived under the assumptions of Higgs-dominance and light neutralinos (notice however that full exact expressions both for the relic abundance $\Omega_\chi h^2$ and for the neutralino-nucleon scalar cross section $\sigma_{\text{scalar}}^{(\text{nucleon})}$ are employed in the numerical evaluations to be discussed in the next Section). Under these hypotheses, the neutralino relic abundance is dominated by the s-wave annihilation in a $\bar{b}b$ pair (unless m_χ is very close to the b -quark mass m_b , in which case the $\bar{c}c$ and $\bar{\tau}\tau$ channel are dominant):

$$\Omega_\chi h^2 \simeq \frac{4 \cdot 10^{-39} \text{cm}^2}{\langle \sigma_{\text{ann}} v \rangle_{\text{int}}} \simeq \frac{10^{-37} \text{cm}^2}{6\pi\alpha_{em}^2} \frac{\sin^4 \theta_W}{\tan^2 \beta (1 + \epsilon)^2} (a_2 - a_1 \tan \theta_W)^{-2} (a_4 \cos \beta - a_3 \sin \beta)^{-2} \frac{[(2m_\chi)^2 - m_A^2]^2}{m_\chi^2 [1 - m_b^2/m_\chi^2]^{1/2}} \frac{m_W^2}{m_b^2}, \quad (4)$$

and the elastic scattering cross section is:

$$\sigma_{\text{scalar}}^{(\text{nucleon})} \simeq \frac{8G_F^2}{\pi} M_Z^2 m_{\text{red}}^2 \left[\frac{F_h I_h}{m_h^2} + \frac{F_H I_H}{m_H^2} \right]^2. \quad (5)$$

In the previous equations we have used the following notations: $\langle \sigma_{\text{ann}} v \rangle_{\text{int}}$ is the integral from present temperature up to the freeze-out temperature of the thermally averaged product of the annihilation cross-section times the relative velocity of a pair of neutralinos; ϵ is a quantity which enters in the relationship between the down-type fermion running masses and the corresponding Yukawa couplings (see, for instance, Refs. [18, 25] and references quoted therein); m_{red} is the neutralino-nucleon reduced mass. The quantities $F_{h,H}$ and $I_{h,H}$ are defined as follows:

$$\begin{aligned} F_h &= (-a_1 \sin \theta_W + a_2 \cos \theta_W)(a_3 \sin \alpha + a_4 \cos \alpha), \\ F_H &= (-a_1 \sin \theta_W + a_2 \cos \theta_W)(a_3 \cos \alpha - a_4 \sin \alpha), \\ I_{h,H} &= \sum_q k_q^{h,H} m_q \langle N | \bar{q}q | N \rangle. \end{aligned} \quad (6)$$

The matrix elements $\langle N | \bar{q}q | N \rangle$ are meant over the nucleonic state. The values adopted here for $m_q \langle N | \bar{q}q | N \rangle$ are the ones denoted by set 1 in Ref. [24]. We remind that uncertainties in the values of $m_q \langle N | \bar{q}q | N \rangle$ can give rise to an increase of the neutralino-nucleon cross section of about a factor of a few [25].

The angle α rotates $H_1^{(0)}$ and $H_2^{(0)}$ into h and H , and the coefficients $k_q^{h,H}$ are given by

$$\begin{aligned} k_{u\text{-type}}^h &= \cos \alpha / \sin \beta, \\ k_{d\text{-type}}^h &= -\sin \alpha / \cos \beta - \epsilon \cos(\alpha - \beta) \tan \beta, \\ k_{u\text{-type}}^H &= \sin \alpha / \sin \beta, \\ k_{d\text{-type}}^H &= \cos \alpha / \cos \beta - \epsilon \sin(\alpha - \beta) \tan \beta, \end{aligned} \quad (7)$$

for the up-type and down-type quarks, respectively.

¹ This is at variance with the results of Ref. [33], where a lower limit on the neutralino mass of 12 GeV has been deduced. Notice that the authors of Ref. [33] consider only the limit of very large m_A , which strongly suppresses processes which involve A -exchange, in particular the neutralino annihilation cross section. On the contrary, we are considering also the light Higgs sector, which is effective in reducing the value of the neutralino relic abundance and therefore in allowing lighter neutralinos (see Eq.(10)).

In the discussion which follows we only wish to establish some correlations implied by the dependence of $\Omega_\chi h^2$ and of $\sigma_{\text{scalar}}^{(\text{nucleon})}$ on the Higgs masses and the neutralino mass. For this purpose we rewrite the two previous expressions as follows:

$$\Omega_\chi h^2 \simeq C \frac{[(2m_\chi)^2 - m_A^2]^2}{m_\chi^2 [1 - m_b^2/m_\chi^2]^{1/2}}, \quad (8)$$

$$\sigma_{\text{scalar}}^{(\text{nucleon})} \simeq \frac{D}{m_h^4}, \quad (9)$$

with obvious definitions for C and D . Here m_h stands generically for the mass of the one of the two CP-even neutral Higgs bosons which provides the dominant contribution to $\sigma_{\text{scalar}}^{(\text{nucleon})}$.

We now consider the case of very light neutralinos, *i.e.* $m_\chi \ll \frac{1}{2}m_A$. Therefore we may further simplify Eq. (8) as

$$\Omega_\chi h^2 \simeq C \frac{m_A^4}{m_\chi^2 [1 - m_b^2/m_\chi^2]^{1/2}} \quad (10)$$

The largest neutralino–nucleon scattering cross sections occur when both m_h and m_A are close to their experimental lower bound ($m_h \sim m_A \sim 90 - 100$ GeV) and $\tan\beta$ is relatively large, in which case also the couplings of Eqs. (6,7) between neutralinos and down–type quarks through h –exchange are sizeable [18]. In this case, from Eqs. (9) and (10) one derives the range of $\sigma_{\text{scalar}}^{(\text{nucleon})}$ at fixed value of m_χ (always in the regime $m_\chi \ll \frac{1}{2}m_A$):

$$\frac{C D}{m_\chi^2 [1 - m_b^2/m_\chi^2]^{1/2} (\Omega_\chi h^2)_{\text{max}}} \lesssim \sigma_{\text{scalar}}^{(\text{nucleon})} \lesssim \frac{D}{m_{h,\text{min}}^4}, \quad (11)$$

where $m_{h,\text{min}}$ stands for the experimental lower bound on m_h . The lower limit to $\sigma_{\text{scalar}}^{(\text{nucleon})}$ displayed in Eq. (11) provides a stringent lower bound on $\sigma_{\text{scalar}}^{(\text{nucleon})}$ for very light neutralinos. This feature will show up in the numerical evaluations presented in the next Section. The upper bound on $\sigma_{\text{scalar}}^{(\text{nucleon})}$ is instead determined by the lower limit on the Higgs mass m_h .

By the arguments given above, it turns out that in the small mass regime ($m_\chi \ll \frac{1}{2}m_A$) the upper bound on the relic abundance $\Omega_\chi h^2 \leq 0.3$ establishes a constraint between the otherwise independent parameters m_χ and m_A (see Eq.(10)).

B. Numerical results

We turn now to the presentation of our numerical results. In Figs.1a–1b we give the scatter plots of the quantity $\xi\sigma_{\text{scalar}}^{(\text{nucleon})}$ in terms of the neutralino mass for different values of the parameter R . The quantity ξ is defined as the ratio of the local (solar neighbourhood) neutralino matter density to the total local dark matter density: $\xi \equiv \rho_\chi/\rho_{\text{loc}}$. In Figs.1a–1b we plot the quantity $\xi\sigma_{\text{scalar}}^{(\text{nucleon})}$, rather than simply $\sigma_{\text{scalar}}^{(\text{nucleon})}$, in order to include in our considerations also neutralino configurations of low relic abundance (*i.e.* cosmologically subdominant neutralinos). We recall that, from experimental measurements of the direct detection rates, only the product $\xi\sigma_{\text{scalar}}^{(\text{nucleon})}$ may be extracted, and not directly $\sigma_{\text{scalar}}^{(\text{nucleon})}$. The quantity ξ is derived here from the relic abundance by the usual rescaling recipe: $\xi = \min(1, \Omega_\chi h^2/[\Omega h^2]_{\text{min}})$, where the minimal value of relic abundance which defines a neutralino as a dominant dark matter component has been fixed at the value $[\Omega h^2]_{\text{min}} = 0.05$. $\Omega_\chi h^2$ and $\sigma_{\text{scalar}}^{(\text{nucleon})}$ are evaluated according to the procedures and formulae described in Refs. [24, 26].

Figs.1a–1b displays quite remarkable properties of the light relic neutralinos from the point of view of their detectability by WIMP direct measurements. These properties are easily understandable in terms of the analytic arguments presented in the previous Section. For instance, in each panel at a fixed value of $R \lesssim 0.1$, there is a characteristic funnel pointing toward high values of $\xi\sigma_{\text{scalar}}^{(\text{nucleon})}$ at small neutralino masses. This originates in the lower bound on $\sigma_{\text{scalar}}^{(\text{nucleon})}$ reported in Eq.(11), which is effective only for very low neutralino masses (below about 15 GeV) and becomes more and more stringent as m_χ decreases. As displayed in Eq.(11), the size of this lower bound, apart from relevant supersymmetric details, is determined by the value of $(\Omega_\chi h^2)_{\text{max}}$, which is set here at the

value $(\Omega_\chi h^2)_{\max} = 0.3$. It is noticeable that at very small values of R , for instance at $R = 0.01$, all supersymmetric configurations are within the cosmologically interesting range of Ω_χ (*i.e.* no configuration of this set is rescaled) and provide large values of $\sigma_{\text{scalar}}^{(\text{nucleon})}$ (*i.e.* large detection rates).

As we increase the value of R , in our scan we are accessing larger values of m_χ : again the largest values of $\xi\sigma_{\text{scalar}}^{(\text{nucleon})}$ are dominated by Higgs–exchange, for Higgs masses close to their lower bound of about 90 GeV. This is also true for the annihilation cross section. This approaches its pole at $m_\chi \sim m_A/2$; therefore, the largest values of $\xi\sigma_{\text{scalar}}^{(\text{nucleon})}$ refer to subdominant neutralinos, as m_χ increases toward $m_\chi \sim 45$ GeV (which represents the pole in the annihilation cross section for the lightest possible A boson). These features are clearly shown in Figs.1a–1b. The panel denoted by “standard” in Fig.1b refers to the usual case of universal gaugino masses: in this case the neutralino mass is bounded from below at about 50 GeV, and therefore all the interesting low neutralino–mass sector is precluded. The last panel in Fig.1b (denoted by “global”) shows our results for R varied in the interval 0.01 – 0.5: the funnel at low masses and the effect of the A –pole in the annihilation cross section are clearly visible.

We recall that, for each panel at fixed R , the lower value of the neutralino mass is a consequence of the experimental bound on the chargino mass, which in turn fixes a lower bound on $M_1 = R \times M_2$. The upper value on the neutralino mass for each panel is a mere consequence of the fact that we scan the M_2 parameter up to 1 TeV.

The detailed connection among the values of $\sigma_{\text{scalar}}^{(\text{nucleon})}$ and those of $\Omega_\chi h^2$ is given in Fig. 2. The strong correlation between $\sigma_{\text{scalar}}^{(\text{nucleon})}$ and $\Omega_\chi h^2$ displayed for $R = 0.01$ reflects the properties of the funnel previously discussed in connection with Fig.1a. All the configurations refer to large values of $\Omega_\chi h^2$: actually, it is the upper bound on the neutralino relic abundance which determines the strong bound on the allowed configurations. By changing R from 0.01 to larger values, we observe that the ensuing increase in m_χ shifts the configurations of largest $\sigma_{\text{scalar}}^{(\text{nucleon})}$ toward lower values of relic abundance, as expected from the analytical considerations of the previous Section. From this figure we see that a fraction of the largest values of the quantity $\xi\sigma_{\text{scalar}}^{(\text{nucleon})}$ refer to dominant neutralinos, while another fraction refers to slightly subdominant neutralinos: $0.01 \lesssim \Omega_\chi h^2 \lesssim 0.05$. Configurations with $\Omega_\chi h^2 < 0.01$, even providing the largest values of the scattering cross section (see, for instance, the panel at $R = 0.04$ in Fig. 2) suffer from a severe rescaling factor ξ which somehow reduces their detectability.

The fact that for small values of R the scattering and neutralino–neutralino annihilation cross sections are dominated by Higgs exchange is a consequence of two facts: the relatively small values for the lower bounds on m_h and m_A and the neutralino composition, which, even though dominated by the bino component, nevertheless possesses a non negligible higgsino contribution allowing the neutralino to efficiently couple with the Higgs fields.

Fig. 3 shows that for small values of R (small m_χ) the neutralino–neutralino annihilation cross-section is indeed dominated by Higgs-exchange diagrams, especially for the largest values of $\sigma_{\text{scalar}}^{(\text{nucleon})}$. The first panel of Fig. 3, which refers to $R = 0.01$, clearly shows that the annihilation cross section is strongly dominated by Higgs exchange. For $R = 0.02$ the annihilation cross section can be either dominated by Higgs or sfermion exchange: however, the configurations which provide values of $\sigma_{\text{scalar}}^{(\text{nucleon})}$ in excess of 10^{-8} nbarn (denoted by crosses) show a clear Higgs dominance in the annihilation cross section. These features are progressively lost when R increases: the annihilation cross section may be dominated by Z exchange (which, by coincidence, has its pole also at about 45 GeV).

Finally, Fig. 4 shows that for low values of R , the neutralino composition is dominated by the bino component, but a deviation from a pure bino composition is present and is mainly due to a mixture of \tilde{B} with \tilde{H}_1^0 . The two composition parameters a_1^2 and a_3^2 remain aligned along the $a_1^2 + a_3^2 = 1$ diagonal line up to $R \sim 0.05$, with a clear dominance (above 70%) in bino. For larger values of R the correlation between a_1^2 and a_3^2 starts to deviate from the diagonal line, a fact that indicates how the two other components are becoming important (it is mainly a_4 which sets up). The panel at $R = 0.1$ shows that the bino component is usually large, but a sizeable mixture starts occurring. The last panel in Fig. 4 recalls the situation for the standard case of universal gaugino masses, where the neutralino may be any mixture of its component fields.

IV. CONCLUSIONS

In the present paper we have focussed our attention on relic neutralinos of light masses: $m_\chi \lesssim 45$ GeV, which are allowed in supersymmetric models where no unification of gaugino masses is assumed. We have shown that these neutralinos may have elastic cross-sections off nucleons which go up to $\sigma_{\text{scalar}}^{(\text{nucleon})} \sim 10^{-7}$ nbarn, with a relic abundance of cosmological interest: $0.05 \lesssim \Omega_\chi h^2 \lesssim 0.3$.

The present upper limits to $\xi \sigma_{\text{scalar}}^{(\text{nucleon})}$ provided by WIMP direct detection experiments [27, 28, 29, 30] do not constrain the supersymmetric configurations for the light neutralinos considered here. This is especially true once the relevant uncertainties (mainly related to the form and parameters of the WIMP galactic distribution function [31] and to the quenching factors for bolometric detectors) are taken into account. The CDMS upper bound [29] could concern a small fraction of supersymmetric configurations in the range around 15 GeV, though very marginally, if the uncertainties on astrophysical quantities are considered. Moreover, the CDMS bound needs a confirmation by a further running in a deep-underground site, as planned by the Collaboration.

The small-mass neutralino configurations analysed in the present paper are accessible to experiments of direct detection with a low-energy threshold and a high sensitivity. An experiment of this type is the DAMA experiment with a mass of $\simeq 100$ kg of NaI(Tl), whose results after a 4-years running show an annual-modulation effect at a 4σ C.L. which does not appear to be related to any possible source of systematics [32]. The DAMA experiment, with its high sensitivity, is potentially good to investigate also the relic neutralinos considered in the present paper.

Acknowledgments

We gratefully acknowledge financial support provided by Research Grants of the Italian Ministero dell'Istruzione, dell'Università e della Ricerca (MIUR) and of the Università di Torino within the *Astroparticle Physics Project*.

-
- [1] J. Ellis, K. Enqvist, D.V. Nanopoulos and K. Tamvakis, Phys. Lett. **B155**, 381 (1985) ; M. Drees, Phys. Lett. **B158**, 409 (1985); Phys. Rev. D **33**, 1486 (1986).
 - [2] M. Drees and X. Tata, Phys. Rev. D **43**, 2971 (1991).
 - [3] K. Griest and L. Roszkowski, Phys. Rev. D **46** 3309 (1992).
 - [4] S. Mizuta, D. Ng and M. Yamaguchi, Phys. Lett. **B300**, 96 (1993).
 - [5] A. Gabutti, M. Olechowski, S. Cooper, S. Pokorski and L. Stodolsky, Astrop. Phys. **6**, 1 (1996).
 - [6] G.Bélanger, F.Boudjema, F.Donato, R.Godbole and S.Rosier-Lees, Nucl. Phys. **B581**, 3 (2000).
 - [7] A. Corsetti and P. Nath, Phys. Rev. D **64**, 125010 (2001).
 - [8] R. Arnowitt, B. Dutta and Y.Santoso, arXiv:hep-ph/0010244.
 - [9] D.G. Cerdeño, S. Khalil, C. Muñoz, arXiv:hep-ph/0105180.
 - [10] V.A. Bednyakov and H.V. Klapdor-Kleingrothaus, Phys. Rev. D **63**, 095005 (2001).
 - [11] H. Baer, C. Balazs, A. Belyaev, R. Dermisek, A. Mafi, and A. Mustafayev, JHEP **0205**, 061 (2002).
 - [12] V. Bertin, E. Nezri and J. Orloff, arXiv:hep-ph/0210034.
 - [13] A. Birkedal-Hansen and B. D. Nelson, arXiv:hep-ph/0211071; Phys. Rev. D **64**, 015008 (2001).
 - [14] A. Bottino, F. Donato, N. Fornengo and S. Scopel, Phys. Lett. **B423**, 109 (1998); Phys. Rev. D **59**, 095003 (1999); Phys. Rev. D **59**, 095004 (1999); Phys. Rev. D **62**, 056006 (2000).
 - [15] A. Colaleo (ALEPH Collaboration), talk at SUSY'01, June 11-17, 2001, Dubna, Russia; J. Abdallah et al. (DELPHI Collaboration), DELPHI 2001-085 CONF 513, June 2001.
 - [16] T. Affolder et al., Phys. Rev. Lett. **86**, 4472 (2001).
 - [17] S. Ahmed et al., (CLEO Collaboration), CONF 99/10, arXiv:hep-ex/9908022; R. Barate et al. (ALEPH Collaboration), Phys. Lett **B 429**, 169 (1998); K. Abe et al. (Belle Collaboration), Phys. Lett. **B 511**, 151 (2001).
 - [18] A. Bottino, N. Fornengo, S. Scopel, Nucl. Phys. **B608**, 461 (2001).
 - [19] A. Bottino, F. Donato, N. Fornengo, S. Scopel, Phys. Rev. **D63**, 125003 (2001).
 - [20] S. Ambrosanio, A. Dedes, S. Heinemeyer, S. Su, G. Weiglein, Nucl. Phys. **B624**, 3 (2002).
 - [21] G.W. Bennett et al. (Muon ($g - 2$) Collaboration), Phys. Rev. Lett. **89**, 101804 (2002); Erratum-ibid. **89**, 129903 (2002).
 - [22] M. Davier, S. Eidelman, A. Höcker and Z. Zhang, [arXiv:hep-ph/0208177]
 - [23] K. Hagiwara, A.D. Martin, D. Nomura and T. Teubner, [arXiv:hep-ph/0209187].
 - [24] A. Bottino, F. Donato, N. Fornengo and S. Scopel, Astropart. Phys. **13**, 215 (2000).
 - [25] A. Bottino, F. Donato, N. Fornengo, S. Scopel Astropart. Phys. **18**, 205 (2002).
 - [26] A. Bottino, V. de Alfaro, N. Fornengo, G. Mignola and M. Pignone, Astropart. Phys. **2**, 67 (1994).
 - [27] For a summary on WIMP direct detection experiments, see, for instance, A. Morales, Nucl. Phys. B (Proc. Suppl.) **110**, 39 (2002).
 - [28] R. Bernabei et al. (DAMA/NaI Collaboration), Phys. Lett. B **389**, 757 (1996).
 - [29] CDMS Collaboration, arXiv:astro-ph/0203500.
 - [30] A. Benoit et al., Phys.Lett. **B545**, 43 (2002).

- [31] P. Belli, R. Cerulli, N. Fornengo and S. Scopel, Phys.Rev. D **66**, 043503 (2002).
- [32] R. Bernabei *et al.* (DAMA/NaI Collaboration), Phys. Lett. **B480**, 23 (2000); Eur. Phys. J. **C18**, 283 (2000).
- [33] G. Bélanger, F. Boudjema, A. Pukhov and S. Rosier-Lees, arXiv:hep-ph/021227.

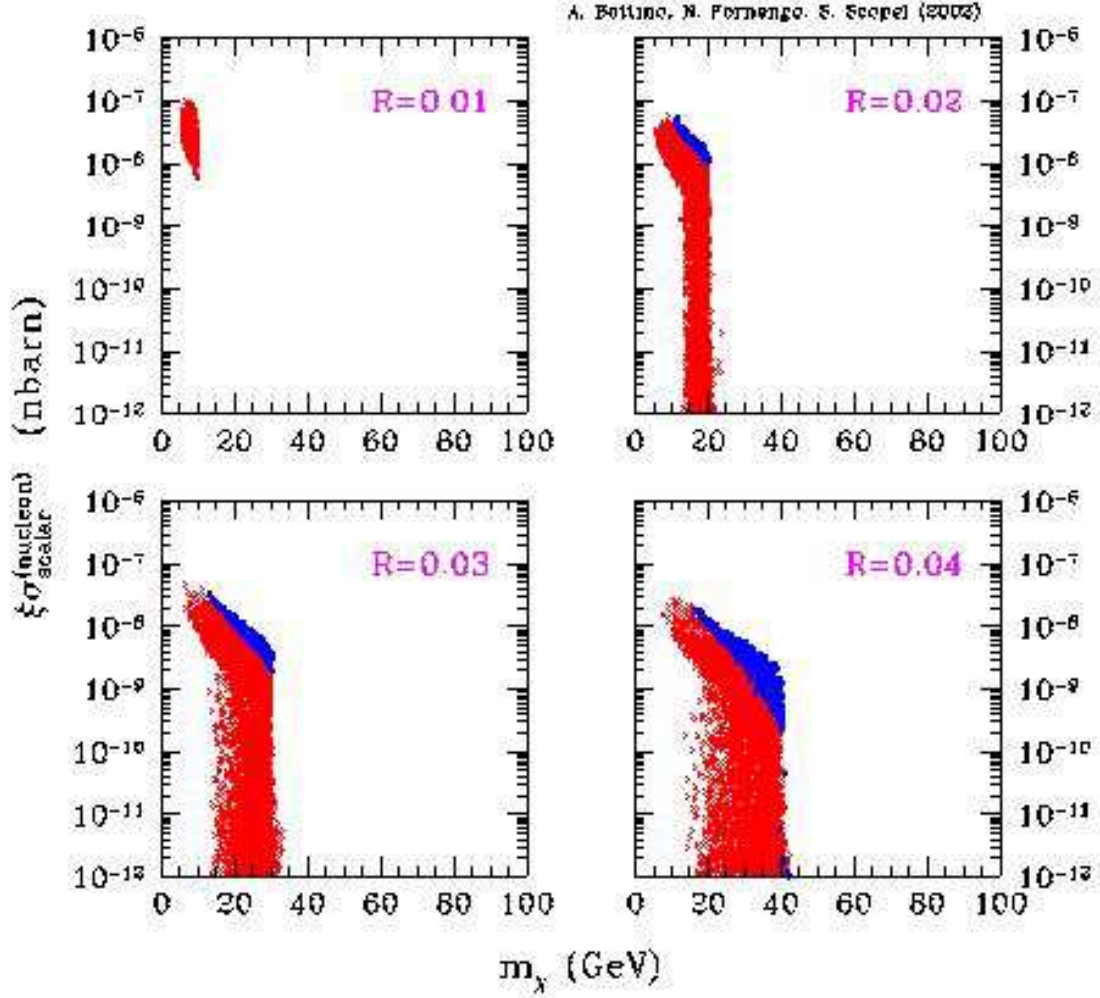


FIG. 1a: Scatter plots of the neutralino–nucleon cross section $\sigma_{\text{scalar}}^{(\text{nucleon})}$ times the rescaling factor ξ vs. the neutralino mass, for nonuniversal gaugino models with different values of the gaugino mass ratio $R = M_1/M_2$: $R = 0.01, 0.02, 0.03, 0.04$. Crosses denote configurations with dominant relic neutralinos ($0.05 \leq \Omega_{\chi} h^2 \leq 0.3$), while dots refer to subdominant neutralinos ($\Omega_{\chi} h^2 < 0.05$).

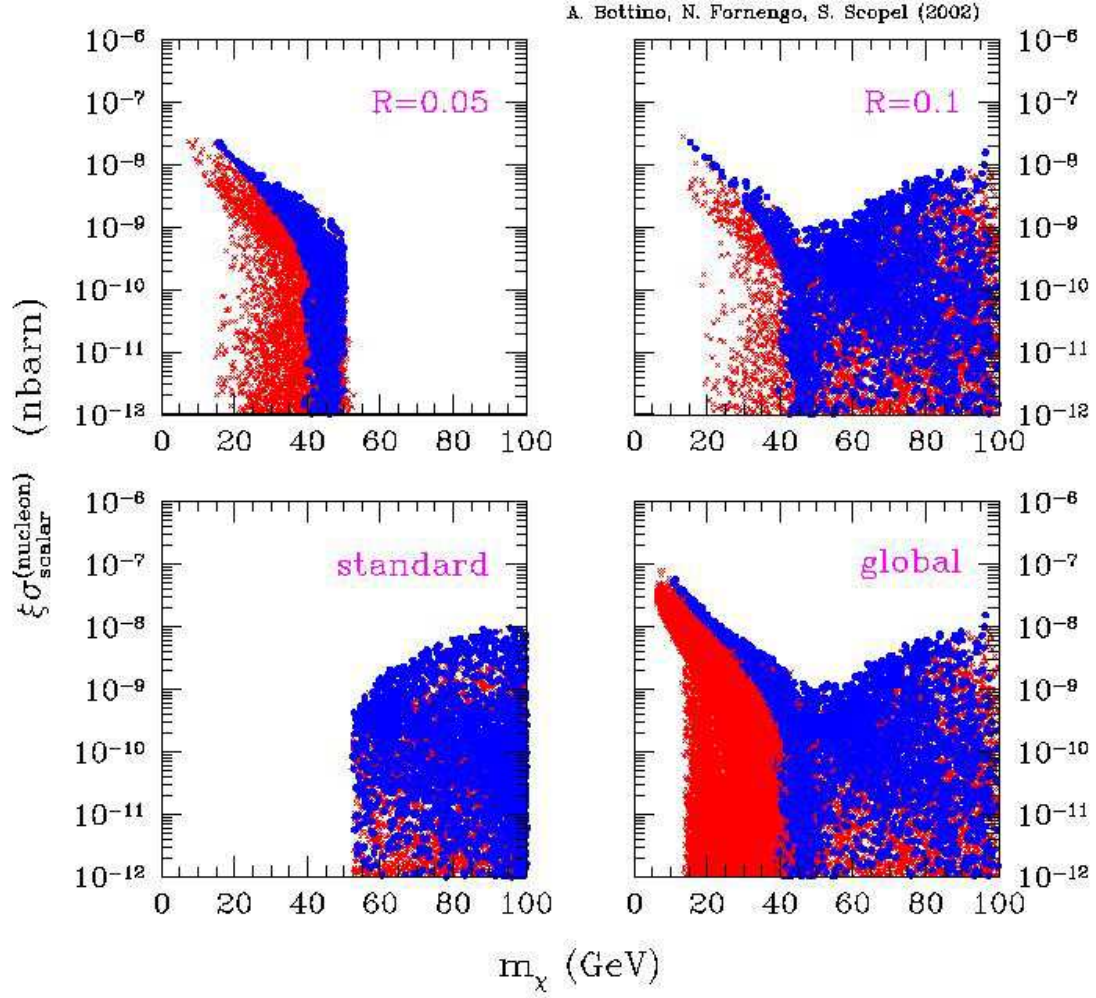


FIG. 1b: The same as in Fig. 1a, for $R = 0.05, 0.1$, for the standard value $R = 5/3 \tan^2 \theta_W \simeq 0.5$ and for a generic variation of R in the interval 0.01–0.5.

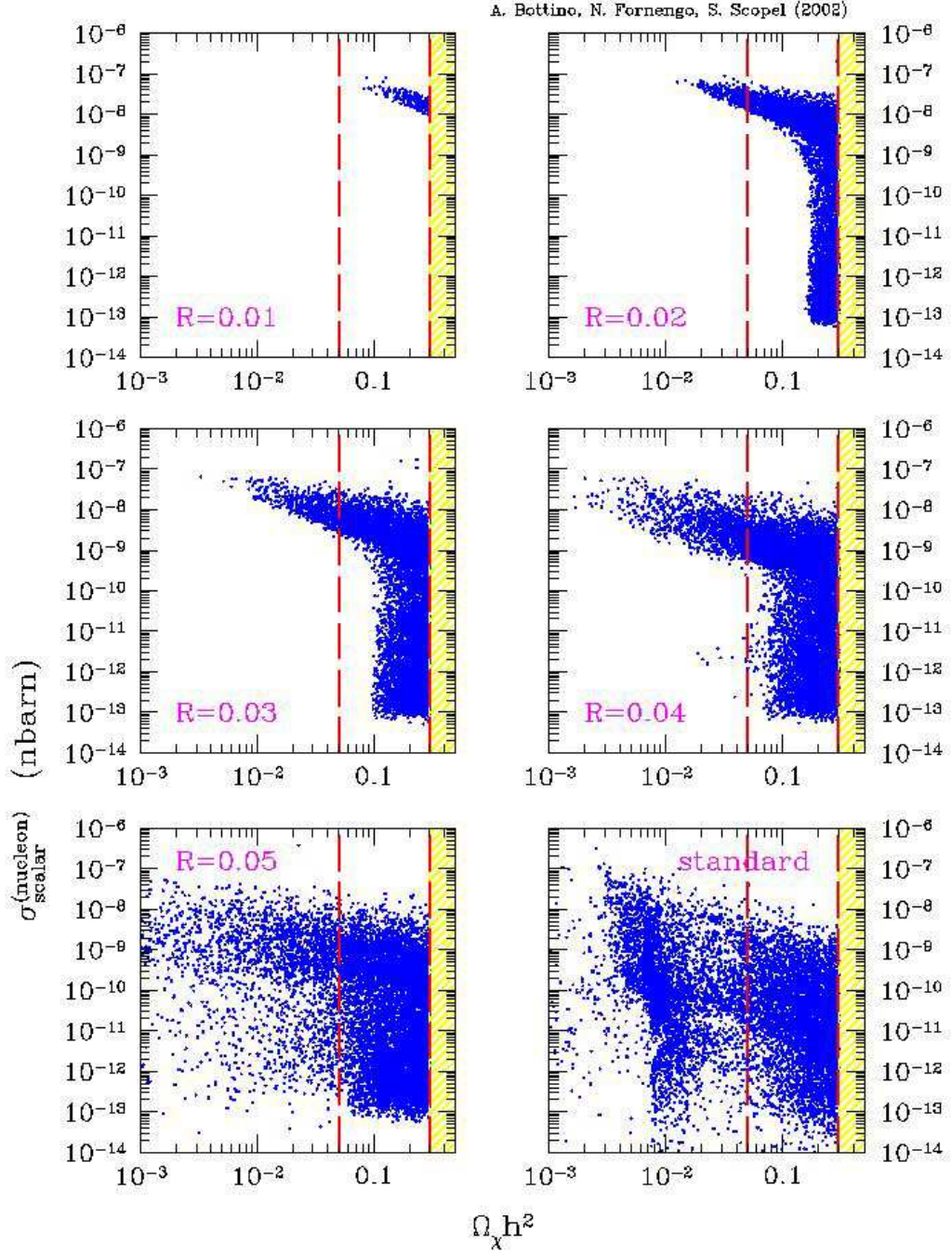


FIG. 2: Scatter plots of the neutralino–nucleon cross section $\sigma_{\text{scalar}}^{(\text{nucleon})}$ vs. the neutralino relic abundance $\Omega_\chi h^2$, for $R = 0.01, 0.02, 0.03, 0.04, 0.05$ and for the standard value $R = 5/3 \tan^2 \theta_W \simeq 0.5$.

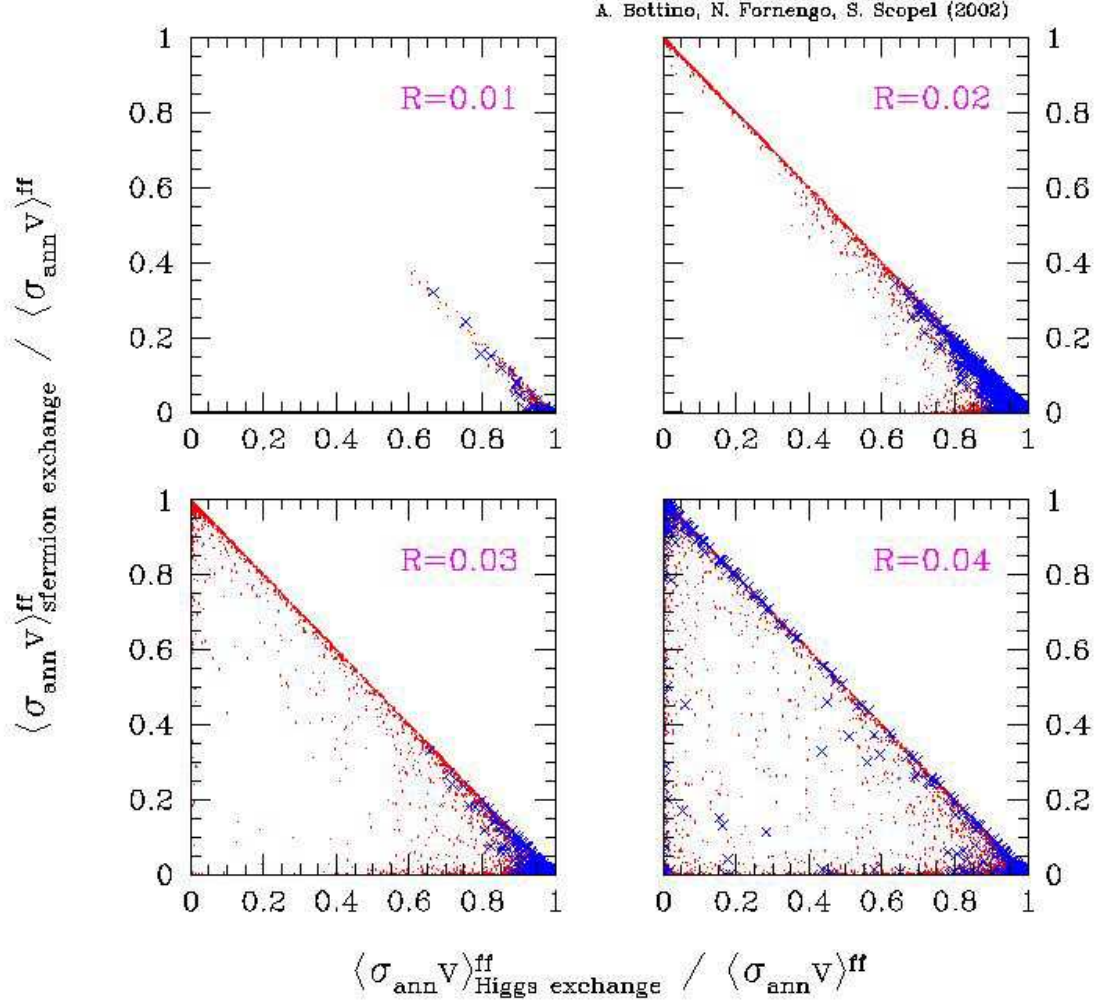


FIG. 3: Scatter plots of the fractional amount of the neutralino pair-annihilation cross section due to sfermion exchange vs. Higgs exchange, for $R = 0.01, 0.02, 0.03, 0.04$. Crosses denote configuration for which the neutralino-nucleon scattering cross section $\sigma_{\text{scalar}}^{(\text{nucleon})}$ is larger than 10^{-8} nbarn.

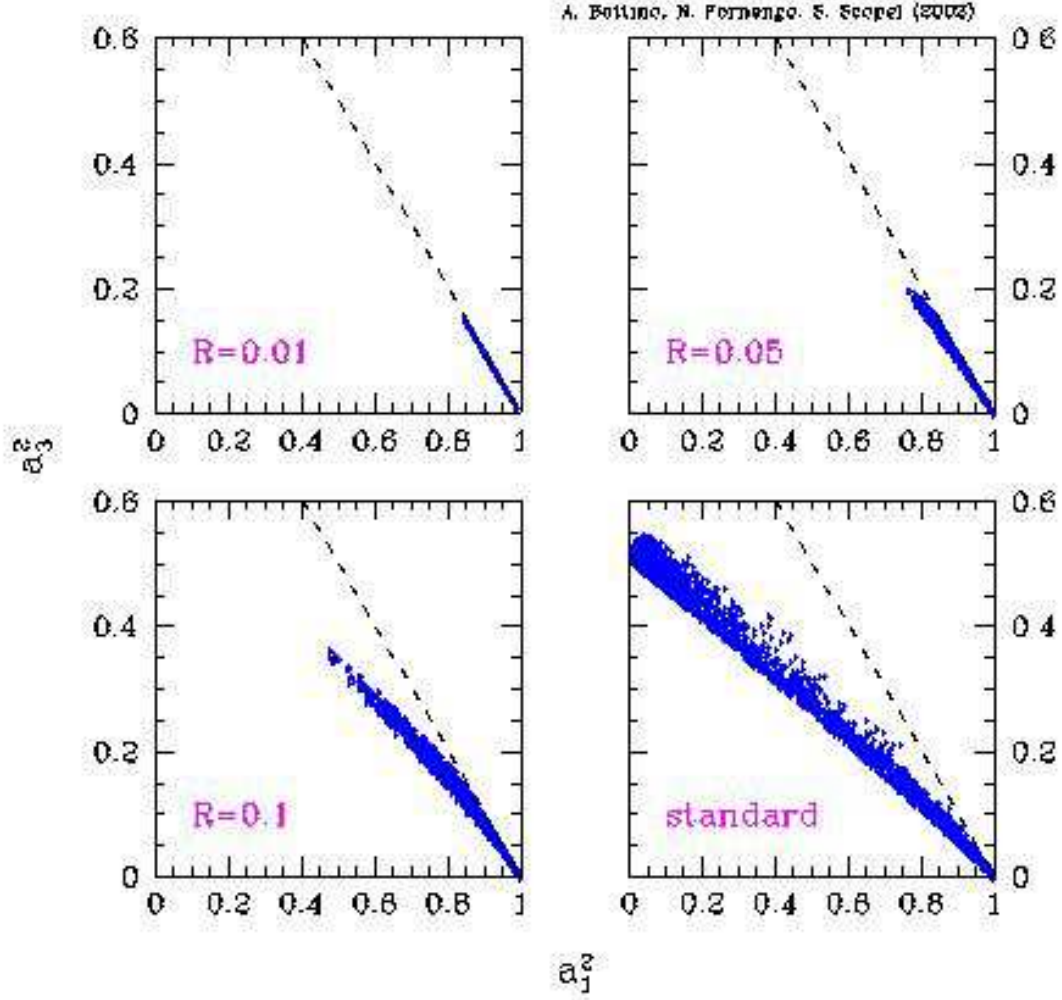


FIG. 4: Scatter plots of the neutralino composition in terms of \tilde{B} (a_1) and of \tilde{H}_1^c (a_3) for $R = 0.01, 0.05, 0.1$ and for the standard value $R = 5/3 \tan^2 \theta_W \simeq 0.5$. The dashed lines denote the line where $a_1^2 + a_3^2 = 1$.